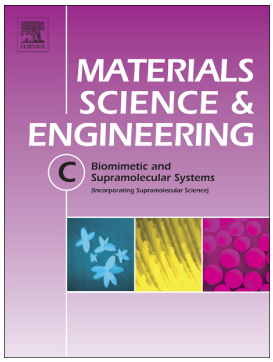

Novel synthesis and structural analysis of zinc oxide nanoparticles for the non enzymatic glucose biosensor

T. Dayakar, K. Venkateswara Rao, K. Bikshalu, V. Rajendar, Si-Hyun Park

PII: S0928-4931(16)31664-2
DOI: doi: 10.1016/j.msec.2017.02.032
Reference: MSC 7366

To appear in: *Materials Science & Engineering C*

Received date: 7 October 2016
Revised date: 29 November 2016
Accepted date: 7 February 2017

Please cite this article as: T. Dayakar, K. Venkateswara Rao, K. Bikshalu, V. Rajendar, Si-Hyun Park , Novel synthesis and structural analysis of zinc oxide nanoparticles for the non enzymatic glucose biosensor. The address for the corresponding author was captured as affiliation for all authors. Please check if appropriate. Msc(2017), doi: 10.1016/j.msec.2017.02.032

Novel Synthesis and Structural Analysis of Zinc Oxide Nanoparticles for the Non Enzymatic Glucose Biosensor

T. Dayakar[a], K. Venkateswara Rao[a*], K. Bikshalu[b], V. Rajendar[c], Si-Hyun Park[c]**

[a]Center for Nanoscience and Technology, Institute of Science and Technology,
Jawaharlal Nehru Technological University Hyderabad,
Telangana State, 500085, India.

[b]Department of Electronics & Communication Engineering, Kakatiya University, Warangal,
Telangana State, 506009, India.

[c]Department of Electronic Engineering, Yeungnam University, Gyeongsan-si
Gyeongsangbuk-do 38541, Republic of Korea

*Corresponding author E-mail: kalagadda2003@gmail.com, Mobile No: +91-9440858664

**Corresponding author E-mail: sihyun_park@ynu.ac.kr, Tel: +82-(0)53-810-3096

Abstract:

A non-enzymatic glucose biosensor was developed by utilizing the zinc oxide nanoparticles (ZnO NPs) synthesized by a novel green method using the leaf extract of *ocimum tenuiflorum*. The structural, optical and morphological properties of ZnO NPs characterized by means of X-ray diffraction (XRD), ultraviolet-visible (UV-Vis) spectroscopy, Fourier transform infrared (FTIR) spectroscopy, scanning electron microscopy (SEM), energy-dispersive X-ray (EDAX) spectroscopy, and transmission electron microscopy (TEM). The XRD analysis revealed that the ZnO NPs were crystalline and had a hexagonal wurtzite structure. The crystallite size measured by XRD was the same as that measured using SEM and TEM. The UV-Vis absorption spectrum estimates the band gap of ZnO NPs present in the range of 2.82 to 3.45 eV. The reduction and formation of ZnO NPs mainly due to the involvement of leaf extract bio-molecular compounds analyzed from the FTIR spectra. The SEM result confirms the morphology of the NPs responsible from the various concentration of leaf extract in the synthesis process. HRTEM analysis depicts the spherical structure of ZnO NPs. The synthesized NPs have the average size ranges from 10-20 nm. The fabricated GCE/ZnO glucose sensor represents superior electro catalytic activity that has been observed for ZnO NPs with a reproducible sensitivity of 631.30μA mM^{-1} cm^{-2}, correlation coefficient of R = 0.998, linear dynamic range from 1~8.6 mM, low detection limit of 0.043 μM (S/N = 3) and response time less than 4 s.

Keywords: Green synthesis, Spherical zinc oxide nanoparticles, Structural properties, Glucose, Non-enzymatic biosensor

1. Introduction

The fast, remarkable sensitivity, high selectivity, stable and low-cost glucose detection finds key role in many fields including clinical diagnosis of diabetes, environment, food industrial analysis, bioprocess monitoring etc., [1]. The

International Diabetes Federation (IDF) estimated about 382 million human being globally has suffered from diabetes in 2013. For diabetic patients the glucose sensors are the leading biggest market for biosensors among the world [2]. Therefore, to avoid diabetic emergencies the diabetic patients test their blood glucose levels in a safe range for numerous instances a day. These measurements are commonly performed the usage of a blood test. Most of the traditional techniques employ colorimetric readout or electrochemical systems. Electrochemical glucose sensor improvement classified into four primary generations. Among them first three generation sensors are enzymatic, which physical parameters limit their practical application and to justify these limitations, an alternative fourth generation glucose sensors based on the direct electro oxidation without the use of enzyme, "non-enzymatic" sensors have been developing [3, 4, 5].

Currently, the improvement of green efficient techniques adopted for the synthesis and characterization of nano particles to explore their applications in scientific and environmental system [6]. By the advancement of a few chemical and physical synthetic procedures, prompts to make utilization of high pressure, energy, temperature and toxic chemical have inconvenient effect at nano scale properties. To overcome these chemical and physical hazards risks, the adoption of green synthesis path has been pursued to minimize bio-hazardous waste, easy reduction of NPs size and shape, cost effective, economically viable, environment friendly, potential medicinal property, faster rate of synthesis and easily scaled up for huge scale synthesis [7,8]. Many researchers established the green synthesis of nanomaterials using plant extracts, microbes and plant parts. The medicinally active plants such as *emblica officianalis*, lemon grass, Aloe vera, Neem have been successfully used for the green synthesis of ZnO, CuO, TiO_2 and Ag NPs, however we used *Ocimum* which much work is not done [9,10,11,12]. Among them ZnO NPs have features such as abundance in nature, excessive electrochemical stability, non-toxicity and biocompatibility, which have immense potential applications in the fabrication of Nano devices [13, 14, 15, 16, 17, 18]. The present research work has been carried out to explore a bio-mediated route for successful synthesis of ZnO NPs with *Ocimum tenuiflorum* leaf extract and applied these NPs in Non-enzymatic glucose sensor phenomena. A validation of the technique were carried out by characterizing the materials, using XRD, UV-Vis, FTIR, SEM, EDAX, TEM and cyclic voltammetry (CV) for elucidating the properties such as structural, morphological and electrochemical and also in order to prove the successful preparation of spherical zinc oxides NPs in their nano. Further, the fabricated enzyme-free glucose ZnO modified electrode was constructed and performed to show a sensitivity of 631.30μA mM^{-1} cm^{-2}. Thus, the ZnO modified electrode achieved desirable glucose sensing ability with excellent long-term stability and high sensitivity thus is very promising non-enzymatic glucose sensor for sustainable application.

2. Materials and Methods

2.1 Chemicals and apparatus

Zinc nitrate hexahydrate (Zn $(NO_3)_2.6H_2O$) analytical reagent grade was purchased from Sigma-Aldrich. All the electrochemical experiments performed by means of Metrohm Auto Lab B.V (JNTUH, India). The three-electrode system consisting of working, reference and counter electrode as a modified glassy carbon electrode (GCE diameter of 3mm) coated with ZnO NPs, saturated Ag/AgCl and Pt wire in a electrolyte of 0.1 M NaOH used to study the electrochemical properties, electrolyte are purged with deoxygenated N_2 gas. The crystallinity and crystal phases

were characterized by using XRD with Bruker D8 X-ray diffractometer (CuKα; λ=1.5418 Å). An optical property of the nano particles were analyzed using Systronics Double Beam UV–Vis spectrophotometer 2202. The elemental composition estimated with energy dispersive spectroscopy (EDAX). The chemical composition was performed by using fourier transform infrared spectroscopy (perkinelmer-FTIR spectrum-100) at wave length range of 450-4000 cm^{-1}. The scanning electron microscopy (SEM JEOL-JSM-7600F) and transmission electron microscopy (TEM) along with selected area electron diffraction pattern (SAED) images were recorded using (JEM-Model 100CX II) to estimate morphological and crystalline properties of samples.

2.2 Preparation of leaf extract and synthesis of the ZnO NPs

Healthy Fresh leaves of *ocimum tenuiflorum* collected and washed with de-ionized water to remove any dust particles and finally air-dried. From that, 25 g of leaves cut into fine pieces and transferred to 500 ml beaker, boiled at 100 ^oC with 100 ml of distilled water. Filtrate of extract collected by using Whatmann's filter paper and stored at 40^oC for further use. Zinc nitrate hexahydrate (Zn $(NO_3)_2$. $6H_2O$) (2mM) solution was made to react with 5ml of the aqueous extract for 3–4 h under continuous stirring at room temperature. After that, the mixture transferred on to hot plat to carry out bio-combustion process. The significance of the bio combustion is to make the mixture into homogeneous and spherical NPs. The resultant products calcined at 450°C for 4 hr. The same above procedure followed for synthesizing the remaining samples by the adding 10, 15 and 20 ml of plant extract and these final products labeled as 5, 10, 15 and 20 ml respectively.

2.3 Fabrication of ZnO/GCE modified electrode

ZnO/GCE modified glucose sensor fabricated by following the simple drop casting method. The polished glassy carbon electrode (GCE) rinsed with alumina powder. Then the adhered alumina was cleaned using ultra-sonicator for about 5 min in ethanol and deionized water. Then the electrode cleaned with water and dried. The ZnO NPs were added to double distilled water with a concentration of 5 mg/ml and then sonicated to have uniform dispersion. From this process, 4µl of NPs coated on GCE and the electrode dried at 35^oC for about 10min in oven. Finally, 2 µl of an aqueous solution of Nafion was dropped on the surface of ZnO/GCE which were dried at room temperature. The electrode active area of bare GCE and ZnO/GCE is 0.0793 cm^2 and 0.23 cm^2 respectively [19].

3. Results and discussions

3.1. X-ray diffraction (XRD)

Fig.1. shows the XRD studies of ZnO NPs prepared by different concentration (5, 10, 15 and 20ml) of *ocimum tenuiflorum* leaf extract. All the XRD peaks of ZnO NPs correspond to hexagonal phase with crystalline wurtzite structure. It was observed that the Nine reflection peaks of 2θ degree with corresponding Miller indices (hkl) values at 31.80° (100), 34.44° (002), 36.28° (101), 47.59° (102), 56.65° (110), 62.92° (103), 68.49 (112), 69.55 (201), and 77.61 (202) and these are perfectly matched with JCPDS card No. 36-1451 and also there is no indication of secondary phase.

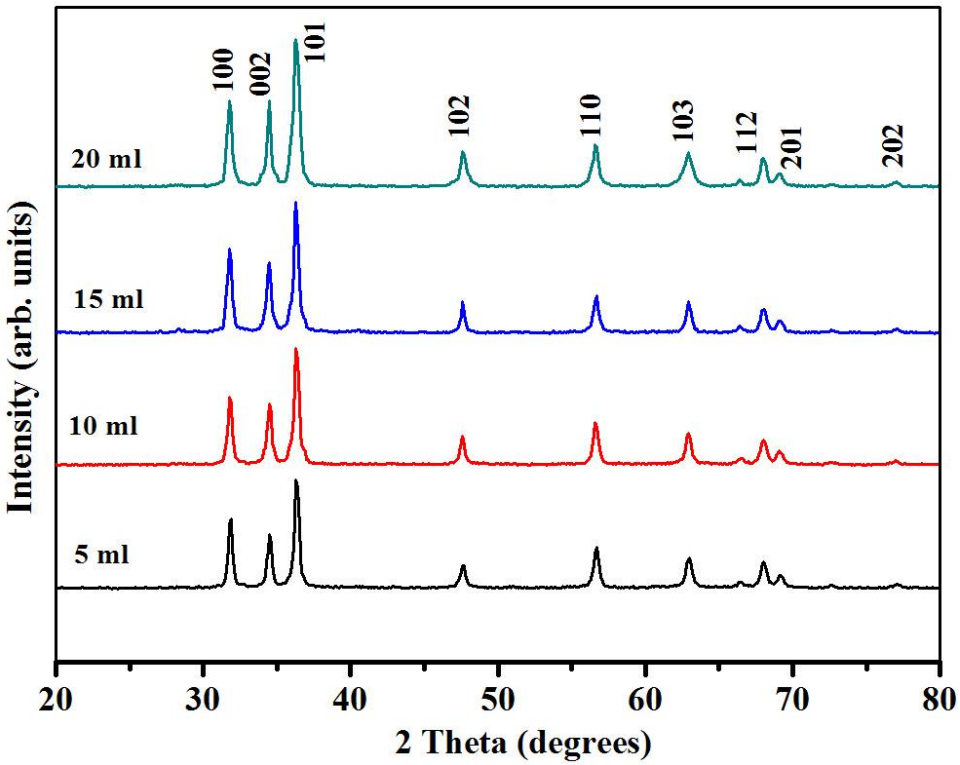

Fig. 1. Shows the XRD of ZnO NPs synthesized with 5, 10, 15 and 20ml of *Ocimum tenuiflorum* leaf extract.

The broadening of XRD peak at half-maximum intensity indicates full width half maximum (FWHM) where used to calculate the average crystallite size of the nanoparticles, and these are estimated from the Scherrer's formula. The concentration of leaf extract affect various structural parameters namely d Spacing, Crystallite size, Strain, specific surface area, dislocation density and Lattice parameters and analyzed with the corresponding equations [20], and the obtained valves from these equations are shown in Table 1.

$$d = \frac{n\lambda}{2\sin\theta} \quad \text{.....1}$$

$$D = \frac{k\lambda}{\beta\cos\theta} \quad \text{..... ..2}$$

$$\varepsilon = \frac{\beta}{4\mathrm{Tan}\theta} \quad \text{..... ..3}$$

$$\delta = \frac{1}{D^2} \quad \text{.....4}$$

$$\beta\cos\theta = \frac{K\lambda}{D} + 4\epsilon\sin\theta \quad \text{.....5}$$

Where *d* is the interplanar spacing, λ is the X-ray -wavelength, *D* is the crystallite size, *θ* is the Braggs angle, β is the full width half maximum (FWHM), δ is the dislocation density, and ε is the micro strain.

Fig. 2 shows the Williamson and Hall (W-H) relation [21] of as synthesized ZnO NPs gives a slope and intercept. Where slope and intercept represents strain (ε) and grain size ($k\lambda/D$) of NPs have x-axis (4 sinθ) and y-axis (β cosθ). A dislocation is an imperfection located inside of a crystal, which strongly affect the nanostructure properties. Present green synthesis method can reduce the dislocations in nanomaterials than the chemical and physical methods, which strongly enhance the properties of ZnO NPs. The dislocation density increase even as the crystallite size decreases with increasing strain [22]. The specific surface area (SA) was estimated using the following relationship, which depends on morphology of sample [23].

$$SA = \frac{6\times10^3}{D.\rho} \quad \ldots\ldots\ldots\ldots\ldots\ldots\ldots\ldots\ldots\ldots\ldots\ldots 6$$

Where, ρ is the density of ZnO (5.606 g/cm^3).

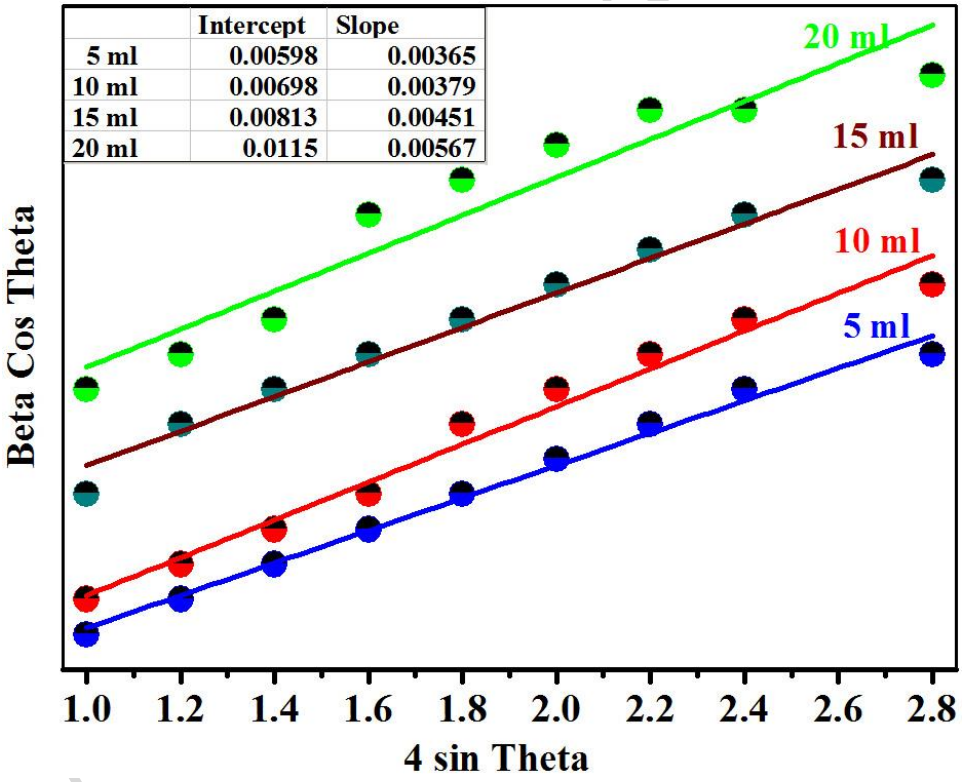

Fig. 2. Shows the Williamson and Hall (W-H) plot of as synthesized ZnO NPs.

Table: 1. Shows ZnO NPs structural parameter obtained from XRD.

d-Spacing (101)	Crystallite size (nm)		Strain	Specific surface area (m^2/g).	Dislocation density	*Lattice parameters	
	Scherrer's	W. H Plots				a =3.232	c= 5.206

5 ml	2.41948	24	23	0.003652	13.4	0.00160	3.279	5.205
10 ml	2.41152	22	19	0.003786	15.1	0.00202	3.275	5.201
15 ml	2.41862	19	17	0.004506	17.2	0.00263	3.276	5.194
20 ml	2.41903	15	12	0.005673	21.2	0.00398	3.272	5.198

*Standard values: a=3.498 and c=5.2066 Å (JCPDS card no. 36-1451).

The lattice constant 'a' and 'c' estimated from the following equation [24].

$$\frac{1}{d^2} = \frac{4}{3}\frac{(h^2+hk+K^2)}{a^2} + \frac{l^2}{c^2} \quad \ldots\ldots\ldots\ldots\ldots\ldots\ldots\ldots\ldots\ldots\ldots\ldots\ldots\ldots 7$$

The calculated lattice constants 'a' and 'c' are very close to that of the standard values (36-1451). These result shows that the lattice constants are not affected much by the green synthesis of ZnO NPs.

3.2. Optical properties

UV–vis spectrum used to estimate the optical absorbance behavior for the ZnO NPs as shown in Fig 3. The absorption peaks observed at the wavelength range of 340-360 nm for all the synthesized samples. Evidently, at the wavelength of less than 400 nm ZnO NPs perform good UV-shielding phenomena, therefore the optical band gap values estimated with the Kubelka–Munk model increased from 2.82 to 3.45 eV as shown in the inset Fig. 3 (inset) and the values are given in table. 2 [25, 26, 27].

$$\alpha h\vartheta = A\left(h\vartheta - E_g\right)^{1/n} \quad \ldots\ldots\ldots\ldots\ldots\ldots\ldots\ldots 8$$

Where α: absorption coefficient, A: constant, h: planks's constant, ϑ: photon frequency, Eg: Energy band gap and n=2 for the direct allowed transitions.

Table.2. shows the optical properties of synthesized ZnO NPs.

	Crystallite size (nm)	**Absorbance (arb.units)**	**Wave length(nm)**	**Band gap E_g (eV)**
5 ml	24	0.22	364	2.82
10 ml	22	0.36	360	3.04
15 ml	19	0.49	352	3.19
20 ml	15	0.58	344	3.45

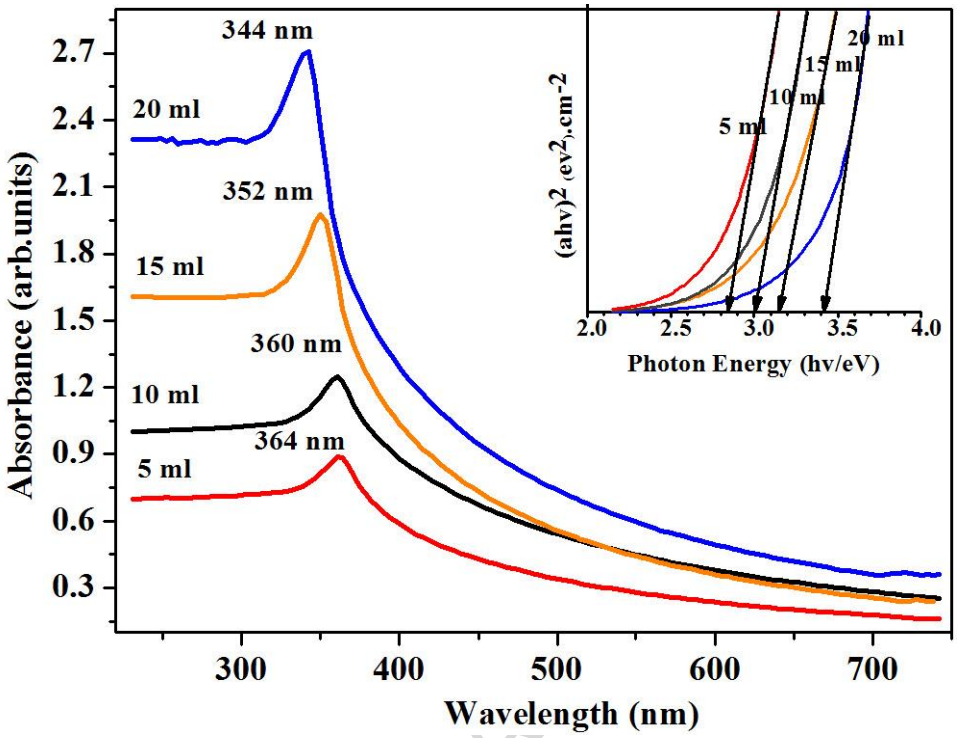

Fig. 3. UV-Visible spectra of ZnO NPs (Inset: Energy band gap diagram)

3.3. FTIR analysis

The FTIR spectra for the ZnO NPs prepared by different concentration (5-20ml) of leaf extract as shown in Fig. 4. Stretching vibrations of Zn–O sharp peak appearing in the range of 450–800 cm^{-1} [28]. The O–O bonds assigned at 1022 and 1114 cm^{-1}, C=O stretching mode appeared at 1365 cm^{-1}. It is important to mention here that the concentration of leaf extract increases the surface to volume ratio increases; therefore, the position of the peak gradually shifts towards the lower wave number then there is an increase in the transmittance percentage [29].

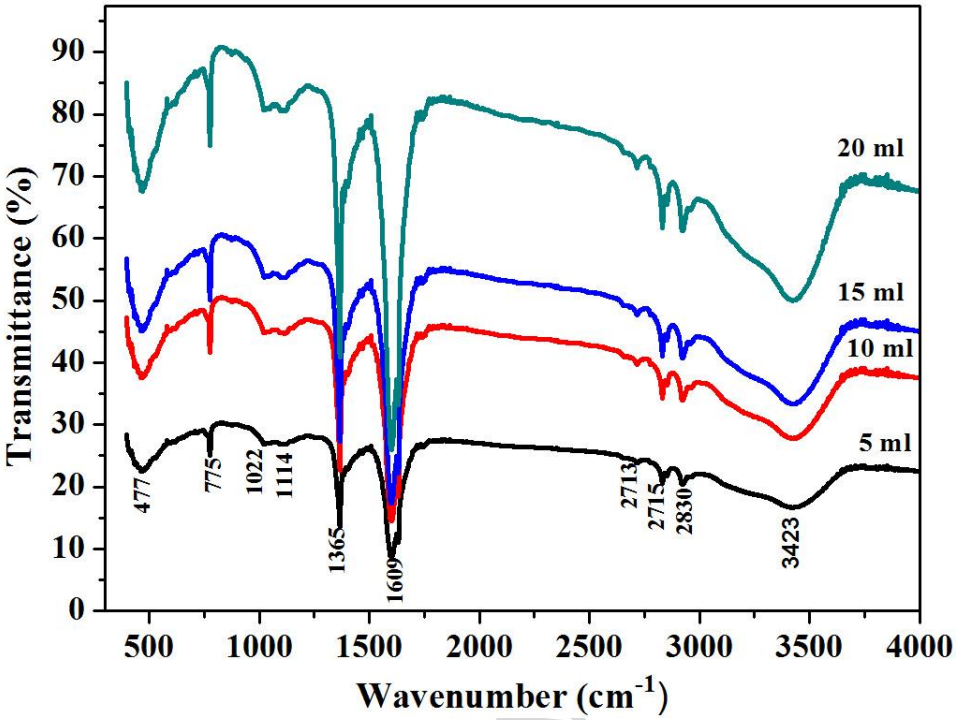

Fig. 4. FTIR spectra of as synthesized ZnO NPs.

The peaks at 2713, 2715 and 2830 cm^{-1}related to C-H bonds, which confirm the bio-molecules adsorbed on the surface of ZnO NPs [30]. The wide band in the region of 1609 and 3423 cm^{-1}due to the presence of hydroxyl group indicating the adsorption of H_2O on to the sample surface [31]. However, the biological entities possess capping and stabilizing agents in the synthesis process such as phytochemicals like flavonoids, phenolics, terpenoids, cofactors, etc. mainly act as reducing and stabilizing agents during synthesis. Flavonoids are a large group of polyphenolic compounds, which can actively chelate and reduce the nanoparticles. The transformation of flavonoids from the enol- to the keto-form, that plays a key role in the formation of Zn^{2+}. Moreover, the internal mechanism of the conversion of ketones to carboxylic acids in flavonoids is likely to be involved in reduction. Interestingly, some flavonoids are able to chelate metal ions with their carbonyl groups, which chelate Zn^{2+}metal ions. The presence of such mechanisms may indeed explain the ability of flavonoids to be adsorbed onto the surface of a nanoparticle. This probably means that they are involved in the stages of initiation of nanoparticle formation (nucleation) and further aggregation, in addition to the bioreduction stage"[32].

3.4. Scanning Electron Microscope (SEM)

SEM images depicts the surface morphology of the ZnO NPs. Fig. 4 (a-d) shows typical SEM analysis of ZnO NPs synthesized from 20 ml of leaf extract. The ZnO NPs have been synthesized in large quantity, which was confirmed, by the higher (1µm) and lower (200 nm) magnifications of SEM image shown in Fig. 4 (a) and (b). Due to high-density growth, most of the NPs possess spherical shape with an agglomerated and well distribution. Moreover, the NPs exhibit smooth surfaces due to the green synthesis method.

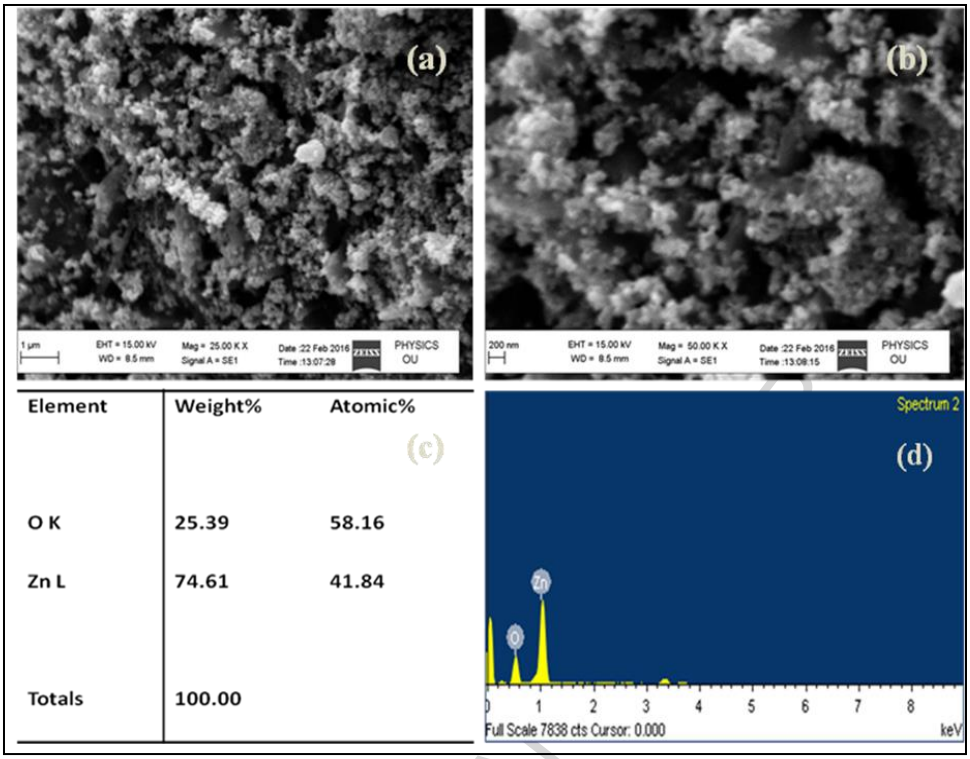

Fig. 4. SEM images of as synthesized ZnO NPs (a) 1 μm magnification (b) 200 nm magnification (c) elemental composition (d) EDAX spectra.

Further analysis of ZnO NPs was evaluated by EDAX in Fig. 4 (c) which confirmed the zinc and oxygen wt% only. The EDAX instrument confirms the detection limits of elements, which show the synthesized ZnO NPs made up by zinc and oxygen only without any noticeable impurity. Further ZnO NPs were analyzed to determine the elemental composition by EDAX spectrum are shown in Fig. 4 (d) which confirms the signal characteristic of zinc and oxygen only. All the presented peaks assigned for Zn and O without any unknown signals proves the purity of ZnO NPs

3.5. TEM analysis

HR (high-resolution) TEM analysis confirmed the morphology and size with their corresponding SAED patterns and lattice parameters of the synthesized ZnO NPs using 20 ml leaf extract concentrations are represented in Fig. 5 (a, b).

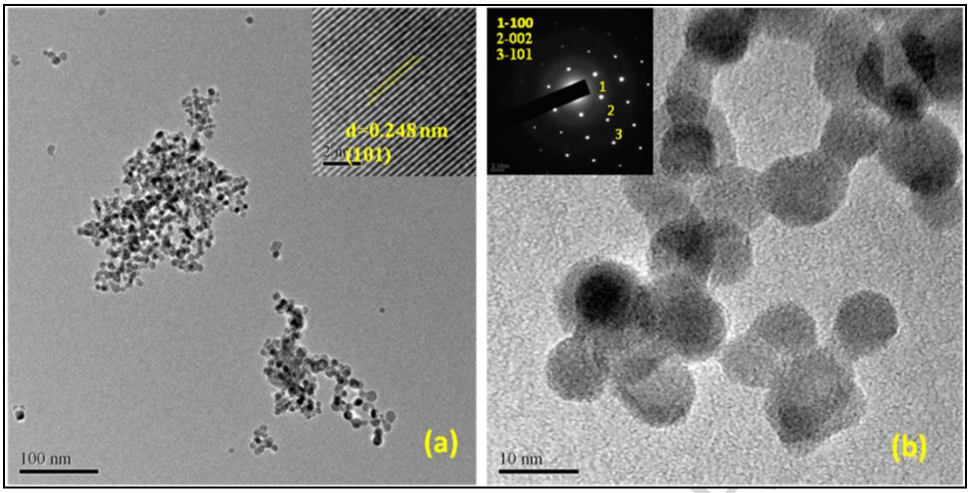

Fig. 5. HRTEM images (a) 100 nm magnification (Inset: interplanar spacing) (b) 10 nm magnification (Inset: SAED patterns) of ZnO NPs with 20 ml *Ocimum tenuiflorum* leaf extract.

The TEM images of ZnO NPs grown in high density, due to that agglomeration obtained and the NPs are in spherical with a narrow size distribution observed in size of 15±5 nm, which are in good agreement with crystallite size obtained from XRD. The distance between two lattice fringes interplanar spacing of as-synthesized ZnO NPs is 0.248 nm that corresponds to the d-spacing of [101] crystal planes as shown in inset Fig. 5(a). The SAED pattern clearly indicate circular concentric circles of three main peaks are well indexed to (100), (002), and (101) planes are suggesting to high crystalline wurtzite hexagonal nanocrystals ZnO NPs are shown in inset Fig. 5(b).

4. Electrochemical characterization

The electro catalytic activities of the 20 ml green synthesized ZnO NPs used as an efficient electron mediator. The working electrode used as modified ZnO/GCE towards glucose oxidation observed at different scan rates. Fig. 6 shows typical Cyclic voltammetric responses for the ZnO/ GCE electrodes was tested at the 5 mV/s scan rate with potential range of 0.2 to 0.9 V (vs. Ag/AgCl) in the supporting electrolyte of 0.1 M NaOH. The glucose electrochemical oxidation for bare GCE electrode surface was difficult to response and the addition of 1mM glucose for the ZnO/GCE electrode shows oxidation and reduction peak potential at 0.68 V and 0.44 V respectively. The reduction peak in the voltammetric responses might be due the reduction of Glucono-δ-lactone [33, 34]. Moreover, this confirms that the ZnO NPs efficiently acts as electron mediator for the electrochemical glucose sensingat different scan rates from 5, 7, 9, 10, 20, 40, 60, 80, 100, 120 and 150 mV/s^{-1}.

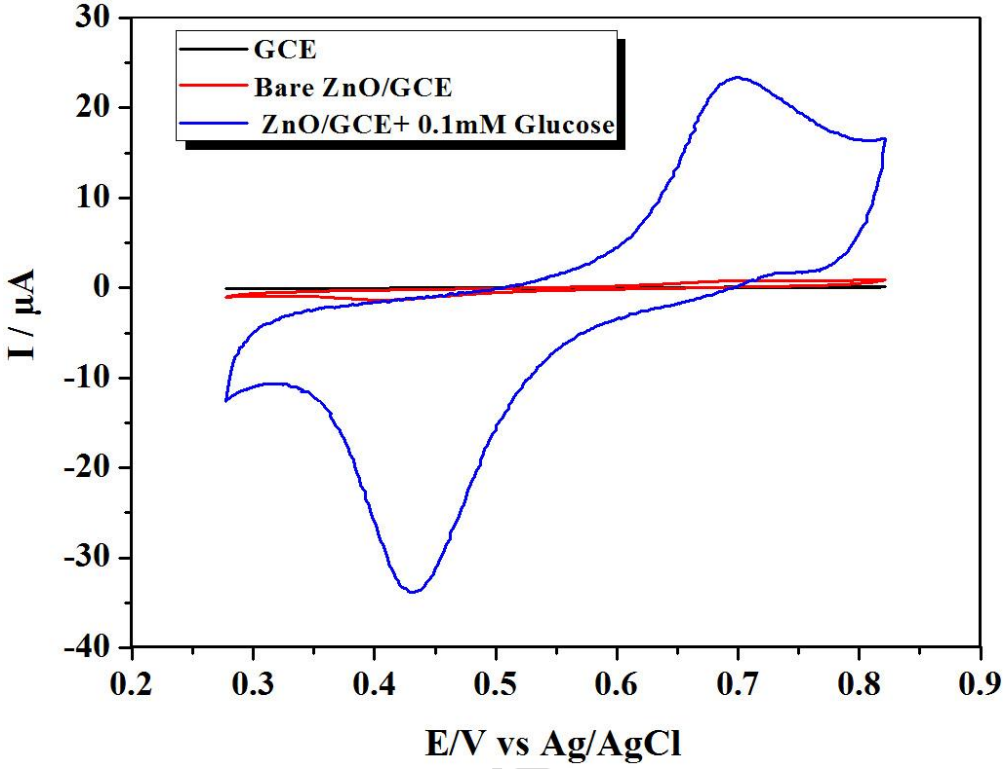

Fig. 6. Shows the CVs of electrodes and in the presence and absence of glucose.

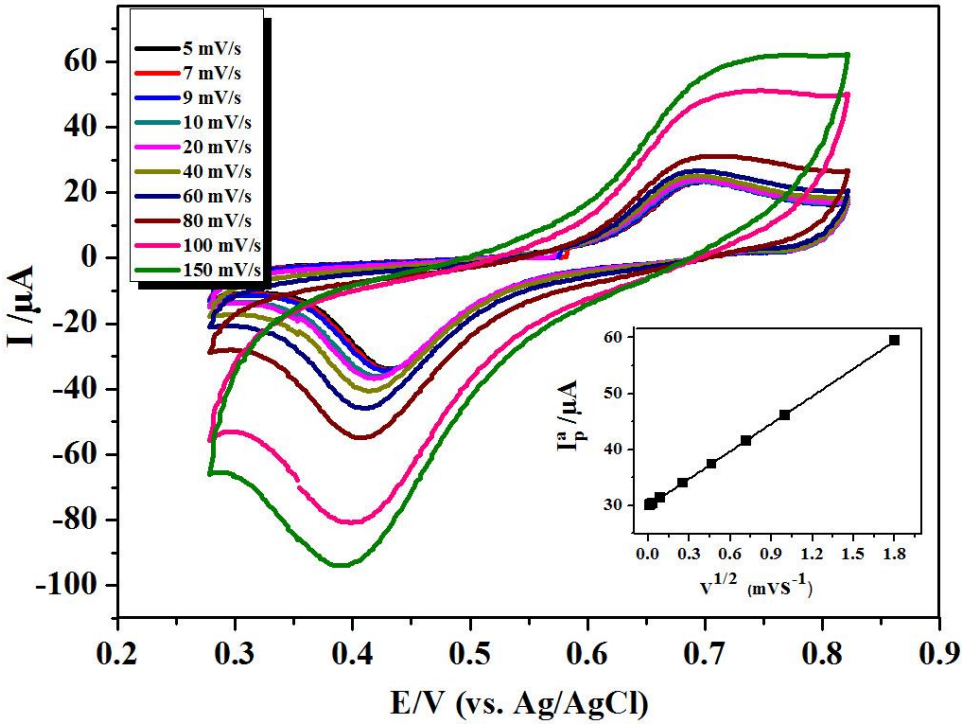

Fig. 7. CVs of ZnO/GCE modified electrode in the presence of 1 mM glucose.

Fig. 7 shows the CVs curve at different scan rates (i.e., 5, 7, 9, 10, 20, 40, 60, 80, 100, 150 mV/s respectively) for the oxidation of 0.1 mM glucose solution against ZnO/GCE electrode. The anodic peak current increases linearly and there is a decrease in the cathodic peak current at the scan rate from 5 to 150 mV s^{-1}, mainly the conversion of glucose to gluconic acid due to kinetic limitation of glucose oxidation reaction which are shown in equation 9 and 10. This is a very rapid and reversible redox reaction performed on the surface of ZnO/GCE modified electrode [35, 36].

$$\text{Glucose} \longrightarrow \text{Glucono-}\delta\text{-lactone} + 2e^- + 2H^+ \qquad \ldots\ldots\ldots\ldots\ldots 9$$

$$\text{Glucono-}\delta\text{- lactone acid} \xrightarrow{\text{Hydrolysis}} \text{Gluconic acid} \qquad \ldots\ldots\ldots\ldots\ldots 10$$

Fig. 7 (inset) shows a plot for Ip vs$V^{1/2}$ in which the anodic peak current shows a linear dependence with square root of scan rates for the ZnO/GCE electrode shows glucose oxidation is a typical diffusion control process over ZnO surface.

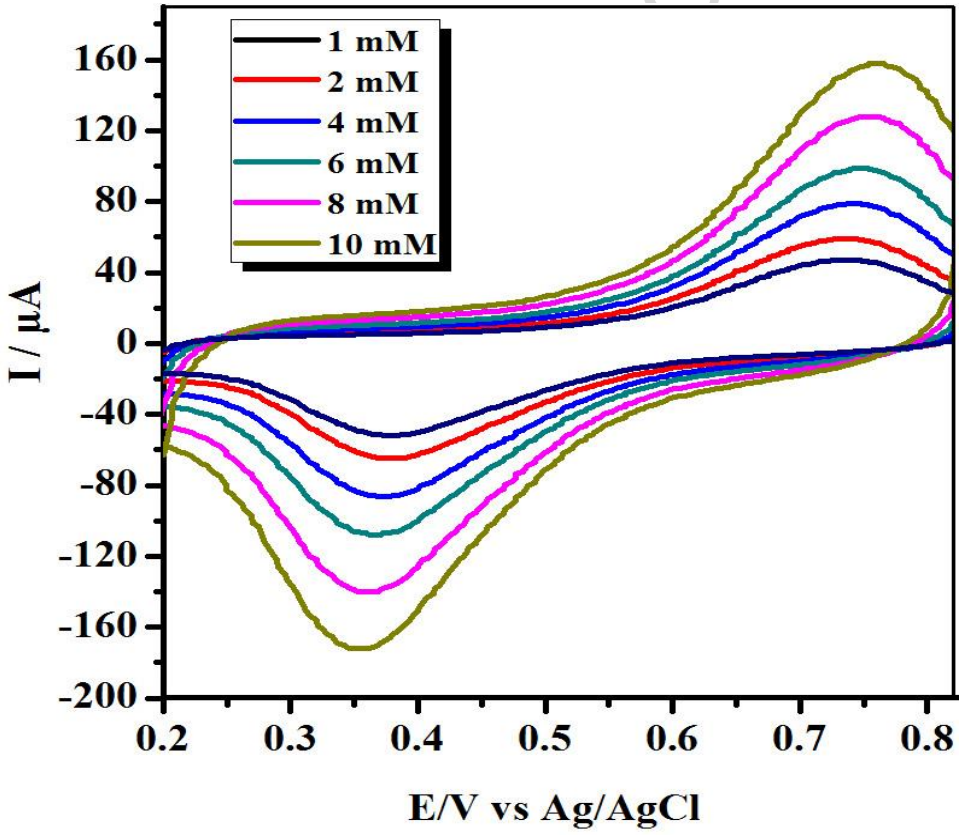

Fig.8. CVs of ZnO/GCE modified electrode in the presence of 1 to 10 mM glucose concentration.

Furthermore, the electron transfer ability between electrolyte and electrode surface with the glucose concentrations ranging from 1 mM to 10 mM investigated using CVs in 0.1 M NaOH solution at 60 mV/s. As shown in Fig 8, electrochemical oxidation of anodic and cathodic peak current is clearly there is a increased and decreased, as the increase in the concentration of glucose and the result suggests the prepared electrode applied for detection of glucose [37].

4.1. Amperometric current-time (i-t) response of ZnO/GCE modified electrode

The ZnO/GCE modified electrode were carried out in 0.1 M NaOH solution at a potential of 0.68 V by the addition of glucose concentration range 1 to 10 mM to estimate the steady state current response as shown in Fig. 9 and the corresponding calibration plot was presented in Fig. 10.

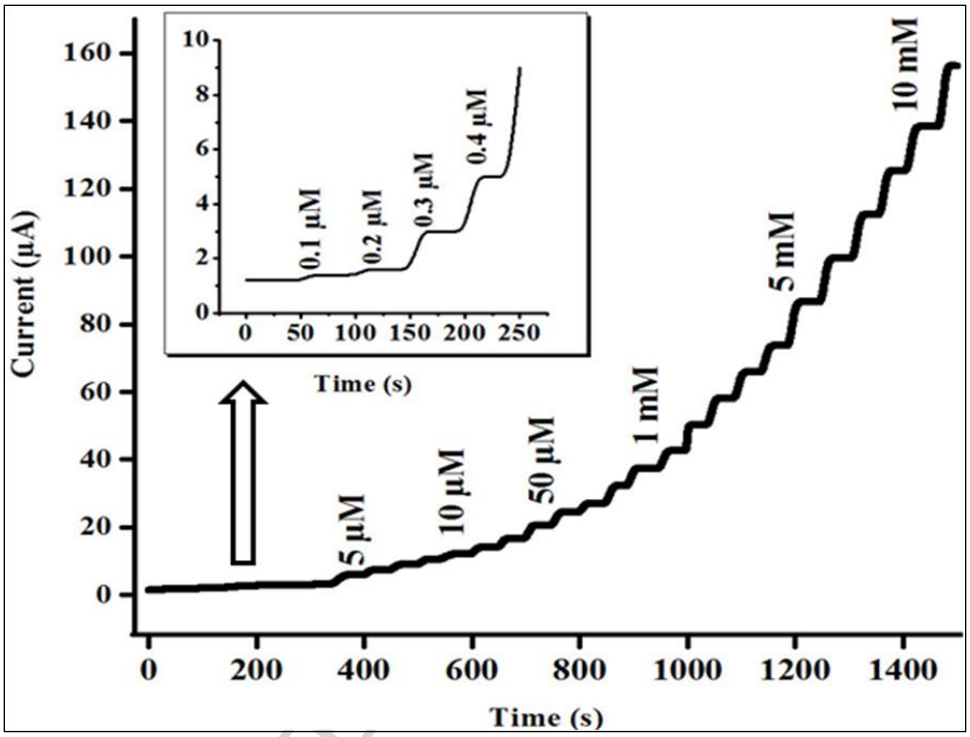

Fig. 9. Steady-state amperometrici-t response of glucose at ZnO/GCE electrode (Inset: 0.1-0.4 μM of glucose)

While increase in glucose concentration, a rapid sensitivity and fast response of step current obtained for ZnO/GCE modified electrode. The high surface area of ZnO NPs makes improved electron transfer with low resistance to decrease the response time. The active sites located on the surface of ZnO NPs are active at low concentration of glucose but the saturation of active site can be seen at high concentration of glucose due to saturation values of current. The i-t current response of glucose at the concentrations of 0.1, 0.2, 0.3 and 0.4 μM as shown in inset fig. 9 [38, 39]. The calibration plots of current response vs. glucose concentration as shown in Fig. 10. In this, the increase in current mainly depends on the concentration of glucose present in the electrolyte solution due to the release of electrons during the electrochemical oxidation of glucose. The calibration plot estimated few analytical parameters namely sensitivity, linear range, low detection limit (LOD) and response time. The slop of calibrated curve and area of electrode gives the sensitivity of ZnO/GCE modified glucose sensor of about 631.30 μAmM^{-1} cm^{-2}, correlation coefficient of R = 0.998, the detection limit were calculated using LOD= (k * sb)/m Where k is chosen as 3; k value 3 corresponds to a confident level of 98.3%. sb is the standard deviation of the blank and m is the calibration sensitivity between concentration vs current. The obtained detection limit is 0.043 mM (S/N=3), linear range of 1 to

8.6 mM with a response time less than 4s. These analytical parameters values are more comparable with other previous report [40, 41, 42, 43, 44, 45, 46, 47, 48, 49, 50, 51], which are given in table 3.

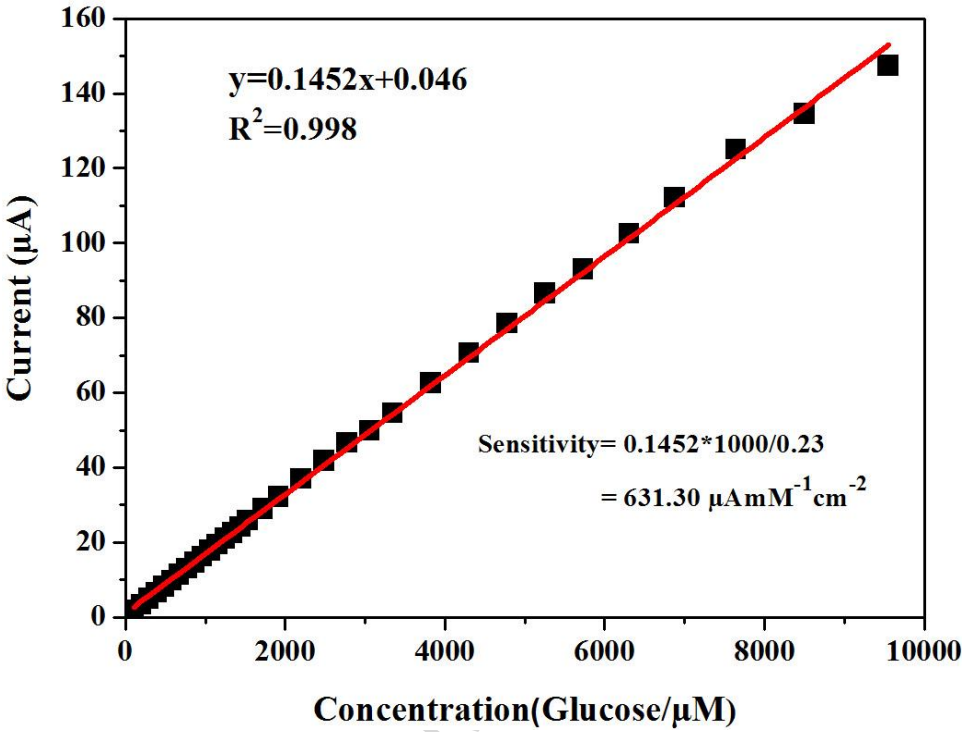

Fig. 10 The calibration plot of steady-state current response vs. concentration of glucose in µM

Table. 3 Comparison of Non-enzymatic glucose sensor parameters for ZnO/GCE modified electrode with previous report modified electrodes.

Electrode materials	**Sensitivity ($\mu AmM^{-1}cm^{-2}$)**	**Response time (s)**	**Linear range(µM)**	**LOD (µM)**	**References**
ZnO-CuO core–shell spheres	1217.4	2	20–4860	1.677	[40]
Mesoporous ZnO-NiO	120.5	3	0.5– 6400	0.5	[41]
NiO hollow microspheres	2390	3	0.00167–6.87	0.53 3	[42]
Nanoporous NiO/TiO_2 layers	252.0	-	0.005-12.1	1.0	[43]
CuO–ZnO nanofibers	463.6	-	0.8–3880	0.126	[44]
Platelet-like $Ni(OH)_2$	202	5–7	0.05–23	6	[45]
Cu–NiO/GCE	0.171		0.5–5000	0.5	[46]

CuO nanoflowers/GCE	2657 1.7	-	1-5 mM	1.71	[47]
CuO–TiO_2 nanotube arrays on Ti foil	79.79	-	1 μM Up to 2 mM	0.5	[48]
NiO–CuO nanowire arrays on Ti	1600	-	0.1–1200	0.42	[49]
CuO–NiO microfibers	3165.53		1 nM 3 μM–	0.51	[50]
CuO and Pt nanostructure/Ta_2O_5 nanoporous honeycomb	160		1 μM Up to 3	1mM	[51]
Green synthesis of ZnO Spherical NPs	**631.30**	**< 4**	**1 to 8.6 mM**	**0.043**	**This work**

4. 2 . Selectivity, Reproducibility and Stability studies of ZnO/GCE modified electrode.

The selectivity studies performed by observing the interfering substances in the blood glucose serum, generally which are easily oxidizable substance such as uric acid, ascorbic acid, lactose, galactose and fructose and contains 30-50 times lower than glucose level. These interfering substances act as distracters for hindering the performance of glucose sensor, so it is important to execute for selectivity studies.

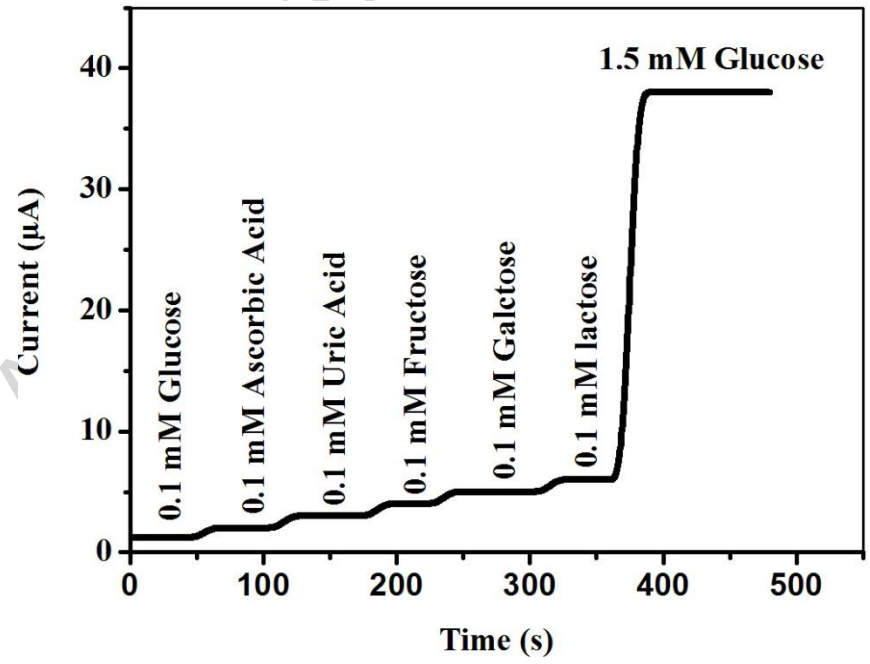

Fig. 11. Amperometric *i*-t response curve for ZnO/GCE to the glucose and interfering substances.

Fig. 11 shows amperometrici-t response for ZnO/GCE with the addition of 1.5 mM glucose solution with increase in 4% current response by the addition of interference substances which depends on physiological concentration [52] and structural difference [53], while there were negligible current response towards the interference substance expect for fructose, galactose and lactose. The possible reason of the negligible influence of Ascorbic acid (0.1mM) and uric acid (0.1mM) is their structural difference with glucose and physiological concentration. However, the modified electrode exhibits obvious current response towards fructose (0.1mM), galactose (0.1mM) and maltose (0.1mM). The results indicate that the ZnO/GCE has an excellent selectivity toward glucose detection. The three different electrodes are prepared in the same procedure to estimate the reproducibility parameter of the ZnO/GCE modified glucose sensor used to detect 6 mM glucose for each electrode respectively. The relative standard deviation (RSD) observed for this measurements was about 2.65 %. The repeatability were tested by conducting the six successive amperometric measurements with one modified electrode at 6 mM glucose concentration and the measured RSD valve is 1.18% and the results indicates the excellent repeatability and reproducibility. The stability were analyzed by placing the electrode at room temperature for 10 days and the difference between the CVs of first and tenth day shows the current response remained 92.7% at 6 mM glucose, makes the good stability towards the glucose oxidation.

5. Conclusions

The ZnO NPs were prepared successfully via Bio mediate process using *Ocimum tenuiflorum* leaf extract. SEM and TEM confirmed the spherical shape ZnO NPs with a particle size of about 15±2 nm. The elemental composition confirmed by EDAX and chemical composition of the NPs by FTIR. The crystalline size, d-spacing, dislocation density and strain of the NPs are calculated by XRD pattern. The fabricated ZnO/GCE modified electrode performed excellent analytical sensor futures such as sensitivity of 631.30 $\mu A\ mM^{-1}\ cm^{-2}$, detection limit of 0.043 mM (S/N=3), linear range of 1 to 8.6 mM with a response time less than 4s, excellent repeatability, reproducibility and stability achieved higher activity towards the oxidation of glucose. Green synthesized NPs performing excellent catalytic activity toward glucose oxidation due to less toxic, smooth surface and decrease of particle size than the chemical and physical synthesized nanostructures. Hence, ZnO NPs act as a sustainable application for Non-enzymatic glucose sensors.

Acknowledgements

One of the authors, Dayakar. T would like to thank their sincere appreciation to the University Grant Commission (UGC), Government of India for financial support through “Rajiv Gandhi National Fellowship (RGNF)” (F1-17.1/2013-14/R GNF-2013-14-SC -AND-41054). The author also thanks Centre for Nano Science &Technology (CNST), Institute of Science &Technology (IST), JNTUH for providing lab and instrumentation facility.

References

[1] S.A. Zaidi, J.H. Shin, Talanta. 149 (2016) 30–42.

[2] R. Prehn, M. Cortina-Puig, F.X. Mu˜noz, J. Electro chem. Soc. 159 (2012) F 134–F139.

[3] P. Lu, Y. Lei, S. Lu, Q. Wang, Q. Liu, Anal. Chim.Acta.880 (2015) 42–51.

[4] N. Hui, W. Wang, G. Xua, X. Luo, J. Mater. Chem. B 3 (2015) 556-61.

[5] G.X. Zhong, W.X. Zhang, Y.M. Sun, Y.Q. Wei, Y. Le, H.P. Pen, A.L. Liu, Y.Z. Chen, X.H. Lin, Sens. Actuators B: Chem. 212 (2015) 72–77.

[6] U.K. Parashar, P.S. Saxena, A. Srivastava, J. anomater. Biostructure 4 (2009) 159-166.

[7] Nadagouda MN, Varma RS, Green Chem. 10(2008) 859–862.

[8] Dar MA, Ingle A, Rai M, Nanomedicine. 9(2013)105–110.

[9] Kumar V, Yadav SK, J Chem Technol Biotechnol. 84(2009)151–157.

[10] Ahmad A, Senapati S, Khan MI, Nanotechnology. 2003 14 (2003) 24– 828.

[11] Basavaraja S, Balaji SD, Lagashetty A, Rajasab AH, Mater Res Bull.43 (2008)1164–1170.

[12] kalimuthu K, Babu RS, Venkataraman D, Bilal M, Gurunathan S. Colloids surf B Biointerfaces 65 (2008) 150-153.

[13] B. Weintrub, Z. Zhou, Y. Li, Y. Deng, Nanoscale 2 (2010) 1573-1587.

[14] J.H. Lee, K. H. Ko, B. O. Park, J. cry. Growth 247 (2003) 119-125.

[15] X. Ma, J. Pan, P. Chen, D. Li, H Zhang, Y. Yang, D. Yang, Opt. Express 17 (2009) 14426- 14433.

[16] Y. Wang, X. Li, N. Wang, X. Quan, Y. Chen, Purif. Technol. 62 (2008) 727-732.

[17] H. Usui, J. Colloid Interface Sci. 336 (2009) 667-678.

[18] Z.H. Wang, J.F. Xia, L.Y. Zhu, F.F. Zhang, X.M. Guo, Y.H. Li, Y.Z. Xia, Actuators B Chem. 161 (2012) 131-136.

[19] Behzad Haghighi, Babak Karimi, Mojtaba Tavahodi, Hesam Behzadneiaehzad Haghighi, Babak Karimi, Mojtaba Tavahodi, Hesam Behzadneia, Materials Science and Engineering C. 52 (2015) 219–224

[20] R. Suresh, V. Ponnuswamy, R. Mariappan, Appl. Surf, Sci. 273 (2013) 457-464

[21] H. B. Premkumar, B.S. Ravikumar, D.V. Sunith, H. Nagabushana, S.C. Sharma, S. Mohandas Bhat, B.M. Nagabhushana, R.P.S. Chakradhar, M.B. Savitha, Spectrochim. Acta, Part A, 115 (2013) 234-243.

[22] M.A. Majeed Khan, Susil Kumar, MaqusoodAhamed, S.A. Alrokayan, M.S. AlSalhi, Nanoscale Res.Lett.6 (2011) 434.

[23] K. Venkateswara Rao, C.S. Sunandana, Journal of Materials Science 43 (2008) 146-154.

[24] R. Anandhi, R. Mohan, K. Swaminathan, K. Ravichandran, Superlatt. Microstruct. 51 (2012) 680-689.

[25] J. Yu, C. Li, S. Liu, J. Colloid Interface Sci. 326 (2008) 433-438.

[26] K.M. Mcpeak, J.B. Baxter, Cry. Growth Design 9 (2009) 4538-4545.

[27] T.P. Rao, M.C.S. Kumar, S.A. Angayarkanni, M. Ashok, J. Alloys Compd. 485 (2009) 413-417.

[28] K. Ravichandran, K. Saravanakumar, R.Chandramohan, V. Nandhakumar, Appl. Surf. Sci.261 (2012) 405-410.

[29] S. Anitha, B. Brabu, D. John Thiruvadigal, C. Gopalakrishnan, T.S. Natrajan, Carbohydr. Polym.87 (2012) 1065-1072.

[30] J. Xie, Y. Li, W. Zhao, L. Biana, Y. Wei, Powder Technol. 207 (2011) 140-144.

[31] J. Singh, P. Kumar, K.S. Hui, K.N. Hui, K. Ramam, R.S. Tiwari, O.N. Srivastava, Cryst Eng Comm 14 (2012) 5898-5904.

[32] Soundarrajan C, Sankari A, Dhandapani P, Maruthamuthu S, Ravichandran S, Sozhan G, Palaniswamy N. Bioprocess. Biosyst. Eng. 35 (2012) 827–833.

[33] S. Ernst, J. Heitbaum, and C.H. Hamann, J. Electroanal, Chem. 100 (1979) 173.

[34] P. Lu, Y. Lei, S. Lu, Q. Wang, Q. Liu, Anal. Chim.Acta.880 (2015) 42-51.

[35] L. Zhang and S. Dong, Electroanal. Chem. 568 (2004) 189.

[36] J. Vilana, M. Lorenzo, E. Gomez, E. Valles, Materials Letters 159 (2015) 154-158.

[37] X. Wang, E. Liu, X. Zhang, Electochim. Acta 130 (2014) 253-260.

[38] K. Tian, S. Alex, G. Siegel, A. Tiwari, Mater. Sc. Eng., C 46 (2015) 548-552.

[39] A. Tarlani, M. Fallah, B. Lotfi, A. Khazraei, S. Golsanamlu, J. Muzart, M. Mirza-Aghayan, Biosens, Bioelectorn. 67 (2015) 601-607.

[40] B. Cai, Y. Zhou, M. Zhao, H. Cai, Z. Ye. L. Wang, J. Huang, Appl Phys. A 118 (2015) 989-996.

[41] Y. Liu, H. Pang, C. Wei, M. Hao, S. Zheng, M. Zheng, Microchim. Acta 181 (2014) 399 1581-1589.

[42] S. Ci, T. Huang, Z. Wen, S. Cui, S. Mao, D.A. Steeber, Biosens.Bioelectron. 54 (2014) 251-257.

[43] Z.D. Gao, J. Guo, N.K. Shrestha, R. Hahn, Y.Y. Song, P. Schmuki, Chem-Eur J, 19 (2013) 15530-15534.

[44] J. Wu, F. Yin, Integr. Ferroelectrics 147 (2013) 47–58.

[45] A. Safavi, N. Maleki, E. Farjami, Biosens. Bioelectron.24 (2009) 1655–1660.

[46] X. Zhang, A..Gu, G. Wang, Y. Huang, H. Ji. B. Fng, Analyst 136 (2011) 5175-5180.

[47] S.Sun, X. Zhang, Y. Sun, S, Yang, X. Song, Z. Yang, Chem. Phys. 15 (2013) 10904.

[48] S. Luo, F. Su, C. Liu, J.Li, R. Liu, Y. Xiao, Y. Li, X. Liu, Q. Cai, Talanta 86 (2011) 157.

[49] R. Ding, J. Liu, J. Jiang, J. Zhu, X. Huang, Anal. Methods 4 (2012) 4003.

[50] F. Cao, S. Guo, H. ma, G. Yang, J. Gong, Talanta 86 (2011) 214.

[51] P.V. Suneesh, K. Chandhini, T. Ramachandran, B. G. Nair, T. G. S. Babu, Biosens. Bioelectrons, 50 (2013) 472.

[52] Ang Gaoa, Xuming Zhanga, Xiang Penga, Hao Wua, Long Baib, Weihong Jin, Guosong Wua, Ruiqiang Hanga, Paul K. Chua, Sensors and Actuators B 232 (2016) 150−157.

[53] Xiangjian Liu, Wenxiu Yang, Lulu Chen, Jianbo Jia, Microchim Acta 183 (2016) 2369–2375.

Graphical abstract

Highlights

- Bio-mediated route has been employed to prepare spherical shape ZnO NPs.
- The Green synthesized ZnO NPs shows excellent electrocatalytic activity toward glucose.
- The sensor shows wider linear range (1~8.6 mM), limit of detection (0.046 μM) and sustainable sensitivity (681.60 μAmM-1 cm-2) toward glucose biosensor.
- Compared to the chemical and physical, Bio-mediated route shows excellent properties for Non enzymatic glucose sensor application.